Cave and Karst Science, Vol.47, No.2, (2020) 93–99
Transactions of the British Cave Research Association

ISSN 1356-191X

Cryogenic features of the permafrost ice caves of Grottedal, northeast Greenland

Hazel A BARTON [1], George J BRELEY [2], Paul TÖCHTERLE [3] and Gina E MOSELEY [3]

[1] Departments of Biology and Geoscience, University of Akron, Akron OH, USA.
E-mail: **bartonh@uakron.edu**

[2] Integrated Bioscience, University of Akron, Akron, OH, USA.
E-mail: **gjb55@zips.uakron.edu**

[3] Institute of Geology, University of Innsbruck, Institute of Geology, University of Innsbruck, Innrain 52, 6020 Innsbruck, Austria.
E-mail: **paul.toechterle@uibk.ac.at**
E-mail: **gina.moseley@uibk.ac.at**

Abstract: The caves of Grottedal, Kronprins Christian Land, northeast Greenland, are found within the continuous Arctic permafrost zone. The caves contain several cryogenic features, including minerals and ice deposits. Convection loops within the air of the caves appear to create a sublimation horizon, above which increasing humidity leads to hoar frost formation. Below this sublimation horizon, dry and desiccating conditions lead to the leaching of $CaCO_3$ and the formation of magnesian calcite and kutnohorite. Evidence of condensation corrosion in these caves may also be responsible for the formation of a new type of cryogenic speleothem (called cryogenic frostwork), which may form from freezing of this condensate on surfaces. Cave-air dynamics, driven by the cold temperatures (measured as low as −17.1°C) and climatic conditions of these permafrost caves, are considered to be responsible for the formation of these observed cryogenic features.

Keywords: Grottedal caves; permafrost; hoar frost; kutnohorite; cryogenic frostwork

Received: 25 April 2020; *Accepted*: 26 May 2020.

Introduction:

Dissolution caves within the Odins Fjord and Samuelsen Høj formations (Llandovery, Silurian) (Smith *et al*., 2004; Smith and Rasmussen, 2020) of Kronprins Christian Land, northeast Greenland (Fig.1), were first described by Davies and Krinsley in 1960. At the time, twelve caves at multiple elevations, with entrances up to 12m in diameter, were identified along a tributary valley in the southern wall of the larger Grottedal (Davies and Krinsley, 1960). The description of speleothems (flowstone and stalagmites) led to a renewed interest in these caves as sites to research the palaeoclimate of this region (Moseley *et al*., 2016). In 2015, an expedition to Grottedal documented a total of 26 caves, where 16 different speleothem samples were collected (Moseley, 2016). U–Th dating and stable isotope analyses revealed that these speleothems provided an important window into the interglacial palaeoclimate of this area (Moseley *et al*., 2016). In addition to speleothems, several other features were identified, including the presence of floor ice, ice crystals, wall-to-wall ice plugs, and extensive hoar frost (Moseley, 2016).

Grottedal is a high arctic desert, situated about 40km to the west of the current edge of the Greenland ice sheet. There are no specific climate records for the valley, but Station Nord (205km to the northeast; Fig.1) has a continuous meteorological record from 1961–1972, with a recorded mean annual surface temperature (MAST) of −17.6°C (IAEA, 2015). According to Needleman (1960), the temperature range in North Greenland is −51 °C to +16°C. The continental position of Grottedal would, however, suggest that it has warmer summer temperatures and cooler winters.

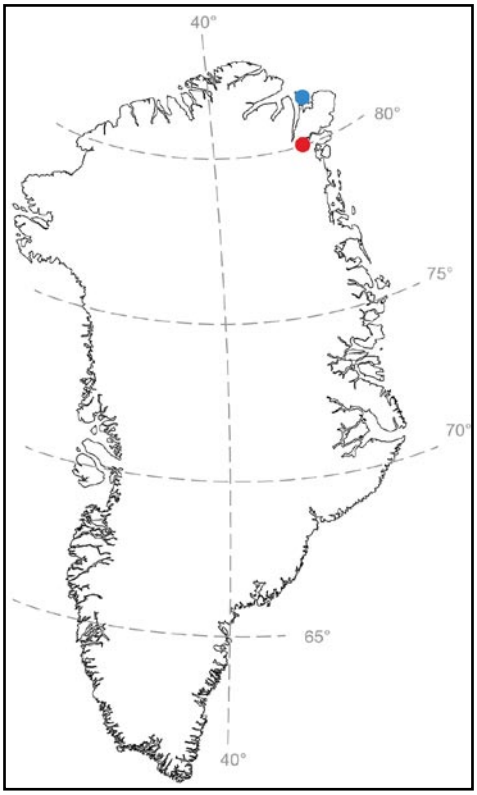

***Figure 1 (right)**: Outline map of Greenland, showing the geographical locations of the Grottedalen Valley (red circle) and Station Nord (blue circle) in the northeast. Major lines of latitude and longitude are provided for reference.*

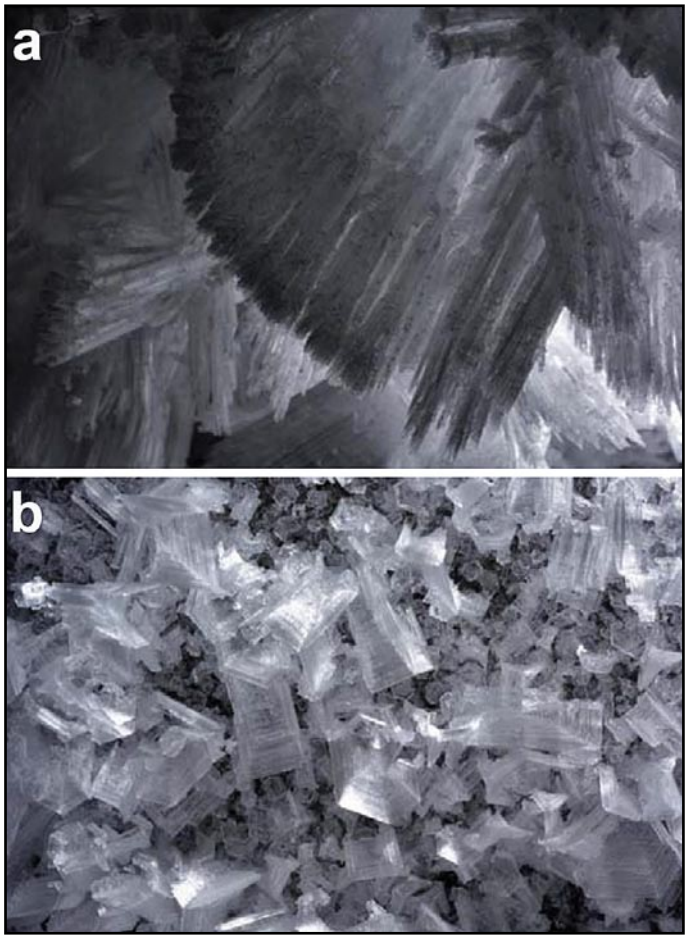

Figure 2*: Hoar frost observed in the Grottedalen caves.*
2a*: Needles of hoar frost on rock surfaces; the needles extended up to 10cm from the rock.* ***2b****: Hexagonal platelet hoar frost, with platelets that locally reach 30cm across, was identified in Crystal Kingdom Cave.*

In May 1960, Needleman recorded mean average daily temperatures ranging from −20°C to +6°C at Centrumsø, with temperatures of −1°C to +14°C in June, and above-freezing temperatures between +2° and +16°C in July; however, seasonal cooling began again in late July, suggesting a small warming window (Krinsley, 1960; Needleman, 1960; Chiron and Loubière, 1988). Additionally, the Greenland Caves Project took spot weather measurements in August 2015 and July 2019 in the Centrumsø and Grottedal region, finding them to be in agreement with previous studies (Donner *et al*., 2020). Surface sediments in Grottedal show extensive patterned ground, indicative of cryogenic activity, and whereas no specific data on permafrost in Grottedal have been recorded, the area lies within the Arctic permafrost zone (Needleman, 1960; Chiron and Loubière, 1988). No cores have been collected to determine the depth of the permafrost in this area, but on the far warmer and much wetter west coast of Greenland (MAST −5.3°C), the permafrost exceeds 150m in thickness (Van Tatenhove and Olesen, 1994; Box, 2002). These data, together with below-freezing temperatures and extensive ice within the caves (Fig.2), indicate that the observed caves are within the continuous permafrost zone (Mavlyudov, 2018).

Ice caves are defined by Harris (1979) as caves where the temperature of the host rock remains below 0°C for more than one season, which leads to the accumulation of ice crystals. This is an important distinction from caves that are formed within ice itself, which are termed glacier caves (Harris, 1979; Luetscher and Jeannin, 2004). Ice caves have unique scientific value because of their ability to preserve palaeoenvironmental and biological material through long-term ice preservation, along with providing an environment for a unique fauna (Lauriol *et al*., 2001; Kern and Perşoiu, 2013; Perşoiu, *et al.,* 2017; Iepure, 2018; Perşoiu and Lauritzen, 2018; Moseley *et al*., 2019). Whereas ice caves have been described at higher elevations worldwide, including in Canada (Ford *et al*., 1976), Romania (Holmlund *et al*., 2005), the European

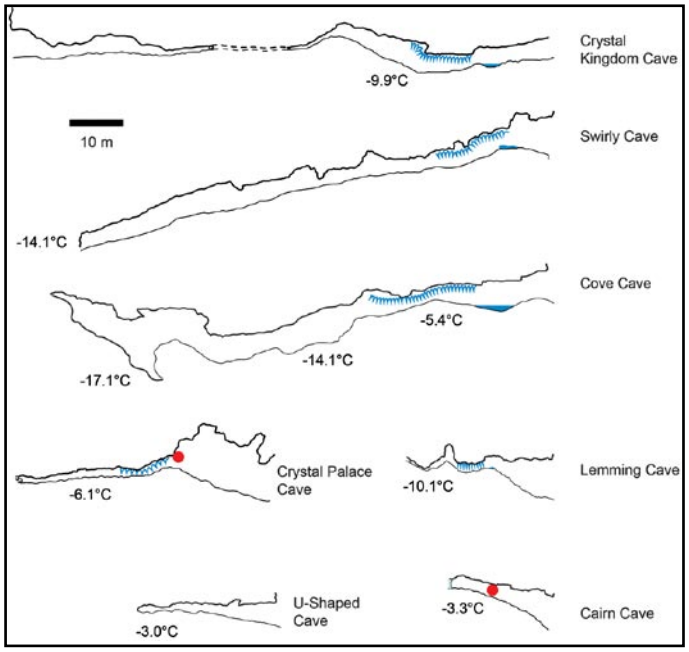

Figure 3*: Profiles of the caves examined in this study, showing measured temperatures at their relative positions of measurement). Locations of floor ice are shown in blue, the extent of hoar frost by the jagged blue lines, and the locations of collected cryogenic frostwork samples are shown by red dots.*

Alps (Luetscher *et al*., 2003), Iran (Soleymani *et al*., 2018), and China (Yang and Shi, 2015), there are limited observations of ice caves within the low-elevation continuous permafrost zone (Ford *et al*., 1976; Clark and Lauriol, 1992; Luetscher and Jeannin, 2004; Lauritzen, 2006; Vaks *et al*., 2013). In this paper, observations are described that were made during a return field campaign to Grottedal in 2019. During this time, new caves were identified, and a more detailed description of their cryogenic features was recorded. These data suggest several features that appear to form under the unusual cave-air dynamics that occur in these permafrost caves (Luetscher and Jeannin, 2004).

Materials and methods

Cave temperatures and humidity were measured using an Extech RH300 digital hygro-thermometer/psychrometer (Extech Instruments, Waltham, MA), which uses the wet bulb method to calculate relative humidity (RH). The RH300 has a resolution of 0.1°C and an accuracy of ± 0.6°C. The psychrometer has a resolution of ±3% RH and an accuracy of 0.1% RH, and it was calibrated in the field at the beginning of the expedition using 33% and 75% standards, with the calibration checked daily.

Whereas the RH300 pyschrometer has a theoretical wet bulb range from −21°C to 100°C, RH measurements in the field could only be taken down to −10°C. To calculate absolute humidity, an air pressure of 950 hPa (equivalent to 510m above mean sea level at 0°C) was used. The online absolute humidity (AH) calculator (**planetcalc.com/2167**) was then used to determine the AH, based on the temperature and the relative humidity for each of the measured sites in the cave profile (Fig.5b). The results are presented as kg of water/m^3.

Thin sections of cryogenic frostwork were prepared by mounting samples of the needle-thin speleothems in Hillquist Thin Section Epoxy C-D resin, and allowing them to cure at 130°C. The samples were then trimmed with a Buehler Isomet low-speed saw, and thin sections were ground to a thickness not less than 200µm using silicon carbide powder of 600 and 1000 grit, and aluminium oxide powder of 1200 grit. Finally the thin sections were polished with Buehler Micropolish 0.3µm Alpha Alumina powder on a Buehler Low Speed polishing wheel.

Rock samples for x-ray diffraction (XRD) were crushed in a PM 100 ball mill (Retsch, Newtown, PA), while the cryogenic frostwork (described below) was crushed in a metal mortar and pestle. XRD was carried out using a Rigaku Ultima IV X-ray

diffractometer, operated at 40KV and 35mA, with a Cu K-alpha energy frequency (wavelength of 1.54Å). Interpretation of diffraction profiles was carried out using PDXL 2.1 software.

Samples for stable isotope ($\delta^{18}O_{cc}$ and $\delta^{13}C_{cc}$; cc refers to calcite) analysis were prepared inside a lamina-flow hood using a handheld dentist drill fitted with a 0.3mm-diameter carbide burr-tipped drill-bit. Samples of 0.15mg to 0.70mg were measured using standard operating procedures (Spötl, 2011) at the University of Innsbruck on a Thermo Fisher DeltaV^{plus} isotope ratio mass spectrometer linked to a GasBench II interface. Analytical precisions are 0.08‰ and 0.06‰ for $\delta^{18}O_{cc}$ and $\delta^{13}C_{cc}$ respectively (1 sigma; Spötl, 2011). All isotope results are reported relative to the Vienna PeeDee Belemnite standard.

Temperature and humidity measurements were recorded from seven caves located within the Grottedal area. The caves are referred to as Lemming Cave (Narlumukaap Qaarsussuaq; Lat: +80.38°, Long: −21.82°), U-Shaped Cave (U-Tut Ilusilik Qaarsussuaq; Lat: +80.38°, Long: −21.74°), Crystal Palace (cave) (Aligoq Illussaarsuaq Qaarsussuaq; Lat: +80.38°, Long: −21.73°), Cairn Climb Cave (Inussuk Innartooq Qaarsussuaq; Lat: +80.38°, Long: −21.72°), Crystal Kingdom (cave) (Aligoq Kunngeqarfik Qaarsussuaq; Lat:+80.41°, Long:−21.68°), Crystal Crawl (cave) (Aligoq Paarnguffik Qaarsussuaq; Lat:+80.41°, Long:−21.68°); Swirly Cave (Sangujoraartoq Qaarsussuaq; Lat:+80.38°, Long: −21.79°); Cove Cave (Eqik Qaarsussuaq; Lat: +80.25°, Long: −21.93°). The names in parentheses are the Greenlandic translation, and neither the English nor the Greenlandic names have been approved officially by the Language Secretariat of Greenland (**oqaasileriffik.gl/place-names**).

Results

Cave temperature

At the cave entrances (below the dripline), at approximately 1.3m above the floor, the cave air temperature responded to external temperature variations, ranging from +4.2°C to +5.6°C in the meroclimate zone of the caves tested (during the expedition, surface temperatures reached +16°C; Donner et al., 2020). The temperatures then dropped quickly to below freezing within a topoclimate zone of only a few metres, with the final ambient temperature depending upon the general shape and size of the cave (Fig.3). In U-Shaped Cave, an essentially horizontal cave with two entrances (Moseley *et al*., 2020), the temperature dropped to −3.0°C, while the short but slightly ascending Cairn Climb Cave had a temperature of −3.3°C (Fig.3). Crystal Palace and Lemming Cave are both quite short – of the order of 50m – (Moseley *et al*., 2020), but accessing the back of these caves required climbing through constrictions and over piles of gravel debris (Fig.3). On the far side of the constrictions, cave-air temperatures fell to −6.1°C in Crystal Palace and −10.1°C in Lemming Cave. These constrictions probably created traps for cold winter air, resulting in the lower cave air temperatures.

Caves with dipping entrance passages, including Crystal Kingdom, Cove Cave, and Swirly Cave (Moseley *et al*., 2020), had far lower ambient temperatures: Crystal Kingdom had a temperature of −9.9°C at the lowest point; Swirly Cave reached −14.1°C; while at the bottom of a pit in Cove Cave −17.1°C was measured (Fig.3). The lower temperatures in these caves are likely the result of density-induced convection or forced advection of colder air into the cave during the winter, whereas the descending passage creates a summer cold air trap (Wigley and Brown, 1976; Smithson, 1991; Covington and Perne, 2015). A diligent literature search failed to find published data recording other ice caves reaching such low temperatures, including permafrost caves in Siberia (lat: +60°), northern Canada (lat: +61° and +67°), and Svalbard (lat: +78°) (Ford, 1976; Ford *et al*., 1976; Lauriol *et al*., 1988; Lauritzen, 2006; Vaks *et al*., 2020).

Hoar frost

The caves that contained the most impressive hoar frost (Cove, Crystal Kingdom, and Swirly) had floor ice inside the entrance. Initially it was presumed that this floor ice formed from residual snow that had blown into the cave and melted, although Lauriol *et al.,* (1988) suggest that such ice is formed through the intrusion of warm air during the summer, melting the hoar frost, which drips to the floor or flows down the walls (Lauriol *et al*., 1988; Gabrovšek *et al*., 2010). In support of this latter hypothesis, the floor ice was transparent, had a smooth, ablated surface, and was associated with ice stalagmites (Fig.4a). If the ice had been formed from snow, it would have been opaque, possibly stratified from diurnal melting/freezing, scalloped by airflow, or contain debris that would blow in with the snow (Luetscher and Jeannin, 2004). Ice floors were also observed deeper into the caves than the immediate entrance zone; in Cove Cave, the floor ice was observed only a few metres from the dripline (Fig.4), whereas in Crystal Kingdom, Swirly, and Lemming caves the ice was at least 10m into the cave (Fig.3). The exception to this pattern was Crystal Crawl, which had extensive hoar frost, but contained scalloped snow (rather than ice) at the entrance (Luetscher and Jeannin, 2004).

In Cove, Lemming and Crystal Kingdom caves, a significant ice horizon could be seen (Figs 4b–d).. Above this horizon, hoar frost was abundant on the ceilings and walls heading into the cave, but below this horizon no hoar frost was observed (Figs 4b–d). Cave climate is known to influence the formation of the hoar

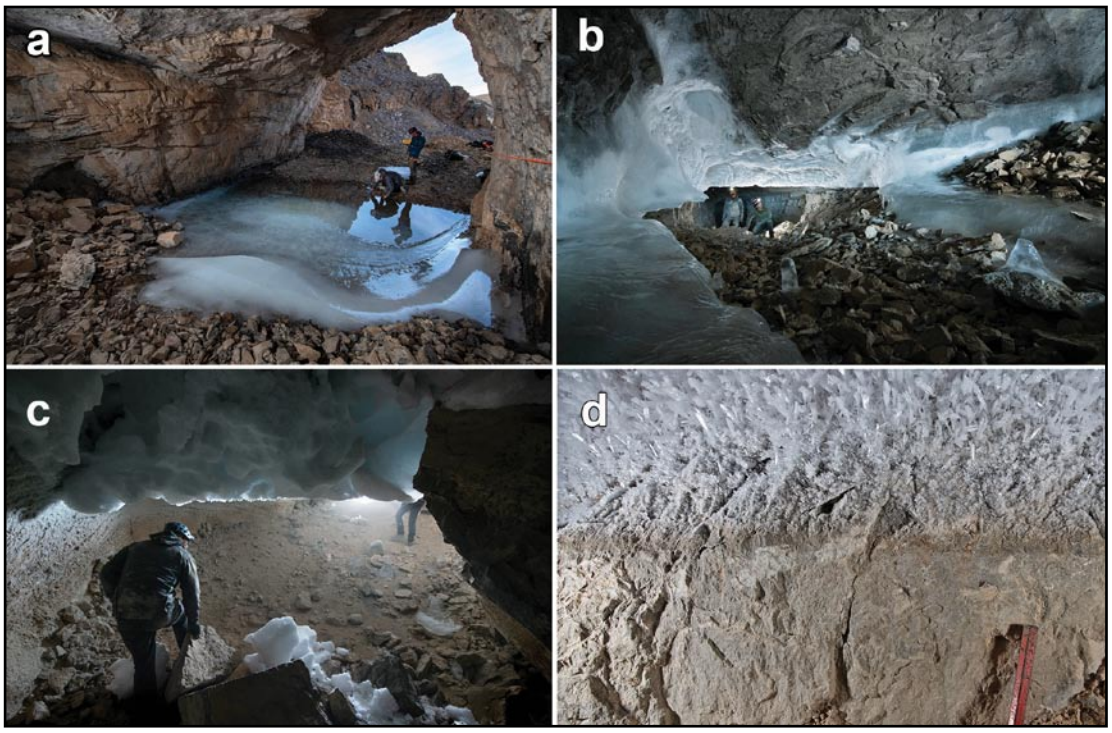

***Figure 4**:*
*The entrance to Cove Cave looking out (**a**), with the floor ice and ice stalagmites, and (**b**) looking in.*
*The hoar frost horizon was particularly distinctive in Cove (**b**) and Crystal Kingdom (**c**) caves, where a dramatic horizon of sublimation was observed on the walls (**d**).*

frost, and whereas this distinct horizon has been observed by other researchers, it has not been described in the literature (D C Ford, personal communication, 2020). Detailed temperature and relative humidity measurements were taken around the hoar frost horizon in Cove Cave (Fig.5). At floor level, the air within the cave was cold (−5.4°C) and dry, ranging from 39.2 – 66.5% RH, depending upon depth into the cave (the RH meter could only record RH values down to −10°C). A 0°C isotherm occurred at 39cm above the floor, where the relative humidity approached 100% (Fig.5b) (Lauriol *et al*., 1988). Above the isotherm (at 1.28m), the air was above freezing (+3.5°C and RH 87.3%), while closer to the ceiling (1.70m) it was warmer (+6.0°C), but the relative humidity had dropped (RH 70.4%; Fig.5b). At the 0°C isotherm, wall ice had created a shelf that protruded up to 30cm into the passage (Fig.5a). This wall ice appears to have formed from the seeping of water from above, but has been carved away underneath, possibly from sublimation of the ice directly to water vapour. The ceilings above the wall and floor ice were essentially frost-free (Fig.5), whereas the hoar frost horizon was observed at approximately the same level as the isotherm (Fig.4).

Ice plugs

Another type of ice formation observed within the caves (specifically Cairn Climb and Lemming caves) were wall-to-wall ice plugs (Fig.6), which were discovered beyond the entrance zone, making it unlikely that they formed from snow blown into the cave. The centres of these ice plugs generally contain trapped air bubbles, making them opaque; however, around the sides the ice is so clear that it is possible to see passages beyond continuing into darkness (Fig.6). In Lemming Cave, one of the ice plugs was found beyond a blocked constriction where the air temperature was measured at −10.1°C, and was transparent for >2m, making it possible to see into a continuing cave passage. In both cases, the ice appeared to be emerging from an existing cave passage, rather than having been formed from the convective freezing/melting of hoar frost. Whereas ice plugs have been described in caves before, these have been formed via occlusion of an existing passage by hoar frost, intrusion of ice from a nearby glacier or from the remnants of a larger deposit that has melted (Wigley and Brown, 1976; Luetscher and Jeannin, 2004; Lauritzen, 2006, Ford and Williams 2007; Perşoiu and Lauritzen, 2018). Intrusive ice has been described only in Castleguard Cave, Canada, where glacial ice has been forced into the cave under pressure (Wigley and Brown, 1976; Ford and Williams, 2007). There are no glaciers directly above the caves in Grottedal; however, it is possible that either water below the permafrost, or super-cooled water created by pressure within the permafrost, entered the passages and froze to create the observed wall-to-wall ice plugs (Pounder, 1965; Luetscher and Jeannin, 2004). The shape of these ice plugs, particularly the one in Lemming Cave, which appeared to be "oozing" out of a passage like an enormous soap bubble, suggests that the ice is being forced out of an existing cave passage (presumably due to the plastic properties of ice under pressure; Pounder 1965). It is unclear whether such ice may be contributing to the enlargement of these passages or, more likely, filling an extant void. Nonetheless, whatever the mechanism, without these ice plugs, some of the caves might have a far larger footprint.

Calcite

Among the features observed in many of the examined caves were small calcite spires that had formed on surfaces near the entrance where the ceiling dipped into the passage, but only on the entrance-side of the hoar frost zone (Fig.7). The calcite spires had a unique morphology (resembling mini-stalactites), were c.7–10mm long and approximately 1–2mm in diameter (Fig.7). This small diameter rules out precipitation by dripping water, which generally produces a minimum speleothem diameter of c. 5mm (the average diameter of a water drop; Hill and Forti, 1997). Given that development of these speleothems occurs at distinct locations, generally on the entrance side of the hoar frost zone, they might be the result of water condensation on rock surfaces warmed by surface air (Gabrovšek *et al*., 2010). Closer examination of the spire material suggested that they were emerging from a film of calcite precipitated on the edge of the ceiling protrusion (Fig.7b). This could suggest that a film of condensing water forms on the rock and moves, via gravity flow, to the lowest point, where the speleothem forms through carbonate precipitation driven by either freezing or evaporation (Gabrovšek *et al*., 2010). Thin sections indicate that the spires are built up in layers (Fig.7c), suggesting that their development is cyclic, although it is unclear whether this would be on a seasonal or diurnal cycle. Each of the layers is of the order of 50–100μm in thickness, with each band of material appearing to form along the length of the speleothem (Fig.7c), possibly supporting capillary water flow along its surface. Bulk XRD analysis revealed that the speleothems comprise aragonite and calcite, likely through initial aragonite precipitation followed by water-driven diagenesis (Domínguez-Villar *et al*., 2017). Given the absence of water in the caves, it was not possible to obtain cave-water samples for chemical analysis; hence it is not known whether impurities (e.g. Mg^{2+}) are involved in polymorph formation. Given the preference for the nucleation of calcite at low temperatures, this is a possibility (Kawano *et al*., 2009).

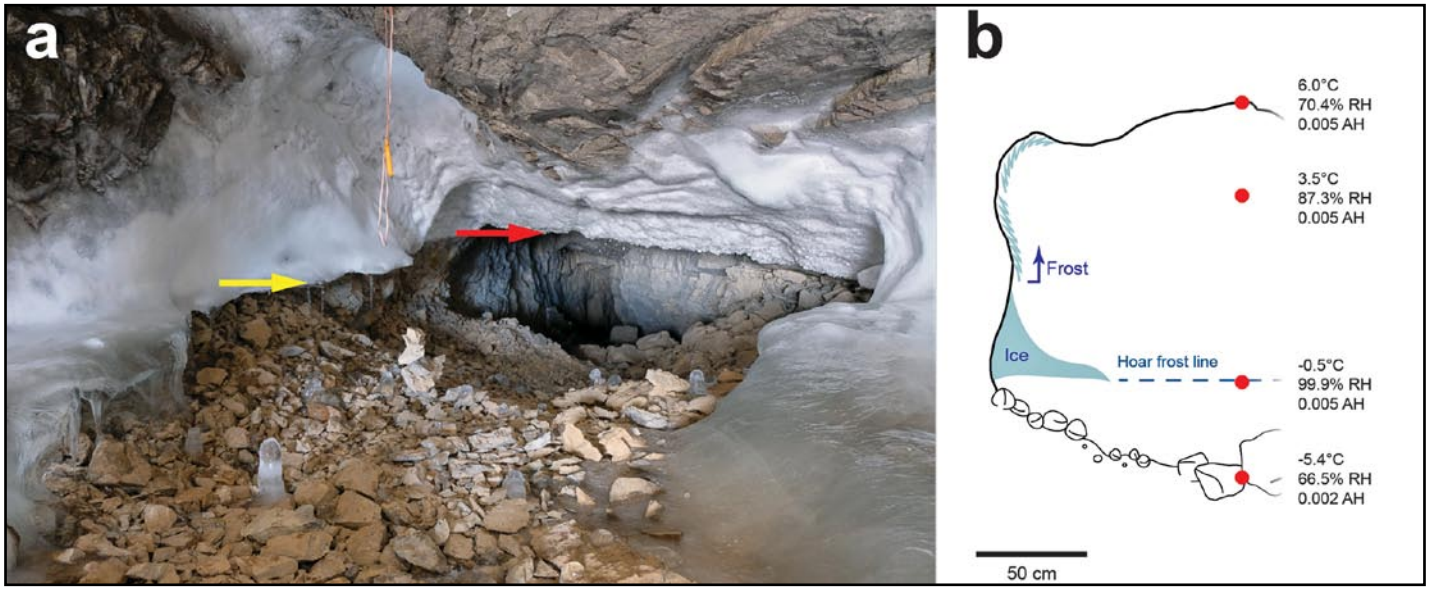

Figure 5*: Location of the temperature and relative humidity measurements in the entrance to Cove Cave.*
5a*: Hoar frost, ice and ice stalagmites in the cave. An ice shelf has formed from water seeping down the wall. A distinct area that has been carved away (yellow arrow) matches a distinct horizon in the hoar frost (red arrow). The temperature/humidity meter is shown hanging in place during measurements.*
5b*: Obtained temperature and relative humidity (RH) values at each location, along with the calculated absolute humidity (AH) in kg/m^3.*

Figure 6*: The ice plug at the back of Cairn Climb Cave. The caver is standing in front of the opaque portion containing air bubbles, and clear ice can be seen at the edges of the plug.*

Water vapour condensing out of the atmosphere can be considered a non-ionic, ideal solution. At 0°–5°C, the dissociation constant (pK_{a1}) for carbonic acid is pH 6.75–6.52 (calculated using the equation of Harned and Davis Jr., 1943), making it aggressive when coming into contact with limestone bedrock (Gabrovšek *et al*., 2010). Mobilization of Ca^{2+} and CO_3^{2-} ions within the limestone will depend upon the amount of dissolved CO_2 in the water vapour (Gabrovšek *et al*., 2010). Solubility of these ions is far lower in ice than in liquid water. Consequently, as the water freezes, ions will accumulate in the residual liquid, CO_2 will off-gas, and precipitation of carbonate minerals will occur (Žák *et al*., 2008). If the process is driven by freezing, these speleothems would represent a previously undescribed form of cryogenic carbonate precipitation (Žák *et al*., 2008). It is unlikely that this process is driven by the freezing of hoar frost, because there would be limited time for the water to reach equilibrium with the rock surface, whilst it leads to precipitation of powdery deposits rather than the observed spike-like speleothems (Harrison and Tiller, 1963; Pounder, 1965; Hill and Forti, 1997).

To determine whether freezing was involved in the development of these speleothems, their stable oxygen and carbon isotope compositions were examined. Isotopic values of 10.77‰ for $\delta^{13}C_{cc}$ and −7.48‰ for $\delta^{18}O_{cc}$ were obtained for the speleothem collected in Cairn Climb Cave (host rock values: $\delta^{13}C_{cc}$ = 0.01‰ and $\delta^{18}O_{cc}$ = −6.08‰), with a $\delta^{13}C_{cc}$ value of 13.01‰ and $\delta^{18}O_{cc}$ value of −8.25‰ for the Crystal Palace speleothem (host rock values: $\delta^{13}C_{cc}$ = 2.7‰ and $\delta^{18}O_{cc}$ −7.3‰). These values suggest fast freezing of a low-ionic-strength solution, and do not correlate with the far lower $\delta^{18}O_{cc}$ values associated with cryogenic cave calcites (Žák *et al*., 2018), or with isotopic values associated with calcite formation via sublimation (Clark and Lauriol, 1992). Given their potential cryogenic development, this new speleothem-type has tentatively been named *cryogenic frostwork*, reflecting its similarity in appearance to frostwork (Fig.7b) (Hill and Forti, 1997).

Other minerals of cryogenic origin

One final observation in the entrances of many caves, beyond the zone of direct light penetration and within the cold (sub-0°C) zone, was a green material, loosely attached to limestone clasts, that was associated with organic debris (such as bird pellets) (Fig.8a). Given the low light intensity in this area, it was unclear whether it was biological or mineral in origin (Fig.8a; Barton *et al.,* 2020). Samples were collected directly from the organic material or a representative clast by scraping off either the surface material (Fig.8b – red dot), or a part of the underlying powdered fragment (Fig.8b – blue dot). As a control, part of the same clast fragment that was buried in the cave sediment was also tested (Fig.8b – green dot). The XRD profiles of the green material were unexpected (Fig.8c); surface and sub-surface scrapings of the clast gave clear signals for low magnesian calcite ($[(Ca_{0.87},Mg_{0.13})CO_3]$ and $[(Ca_{0.97},Mg_{0.03})CO_3]$, respectively), whereas the portion of the clast buried in the sediment had a weaker, but clear, signal for the rare carbonate, kutnohorite ($CaMn^{2+}(CO_3)_2$; Figs 8c–d). None of these minerals is known specifically to be green in appearance (Hill and Forti, 1997), although pale green kutnohorite has been observed in Mont Saint-Hilaire, Canada, and a bone in a South African cave shelter (B Onac, personal communication, 2020). Kutnohorite has previously been seen to form under cold and arid conditions (Georgiadis *et al.,* 2019), and these data suggest an enrichment in the Mg^{2+} content of the material, possibly through the differential solubility of $CaCO_3$ (K_{sp} = 3.3 × 10^{-9} at 25°C) versus $MgCO_3$ (K_{sp} = 1.5 × 10^{-8} at 25°C). Under the observed cold, dry airflow in the caves, $CaCO_3$ and its hydrated variants would leach out of solution first, leading to enrichment in the remaining ions (Harmon *et al*., 1983; Lauritzen and Lundberg, 2000). The pocked surface of the clast (Fig.8b) suggests that it has undergone condensation corrosion, presumably while still attached to the cave wall (D C Ford, personal communication, 2020), which would provide the necessary leaching conditions to enrich in surface Mg^{2+} ions (Lauritzen and Lundberg, 2000). It is unclear how Mn^{2+} would be enriched on the portion of the clast in contact with the sediments, although the sorption of Mn^{2+} to calcite surfaces has been shown to produce kutnohorite at low (µmol) ion concentrations (Middelburg *et al*., 1987). The green material directly attached to the organic matter (Fig.8a) was poorly crystalline, and the XRD signal was somewhat obscured by the organic material itself (Fig.8c), while microscopy suggested the presence of photosynthetic cells. These data suggest that photosynthesis under low-light conditions could be responsible for the observed green colour (Behrendt *et al*., 2020).

Conclusions

Due to the remote location of the field site (Fig.1), the short field season, and difficulty in accessing many of the caves (Moseley, 2016), it is not possible to carry out a long-term climate study of the Grottedal caves. Nonetheless, high-resolution digital mapping permitted the precise location of hoar frost and cave temperature/humidity to be recorded, allowing them to serve as a proxy for the more detailed measurements that would be required for a comprehensive climate study (De Freitas and Schmekal, 2003, Pflitsch *et al*., 2006; Covington and Perne, 2015; Bertozzi *et al*., 2019). As these caves are within the permafrost zone, the bedrock is below 0°C year-round; however, no specific measurements of rock temperature could be made. In the caves without noticeable

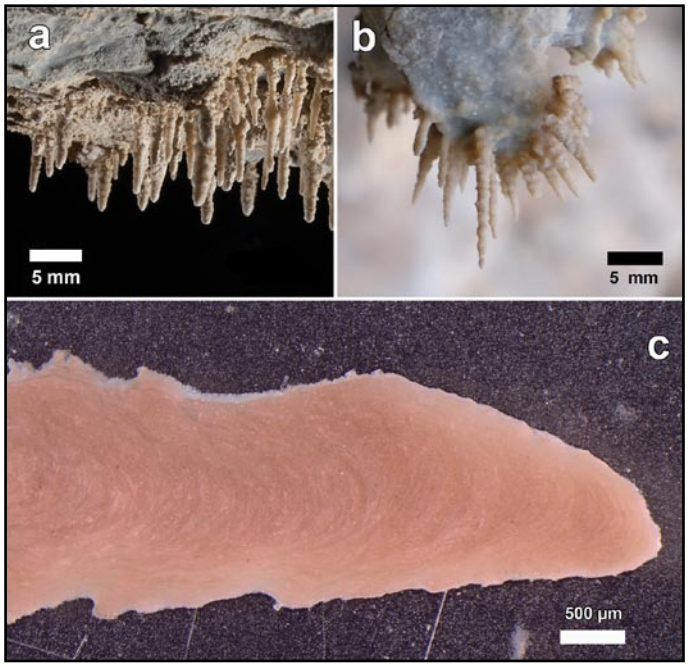

Figure 7*: Cryogenic frostwork found in several of the examined caves.* ***7a****: Cryogenic frostwork below a ledge in Cairn Climb Cave.* ***7b****: A hand sample (collected from Crystal Palace Cave), which was used to generate the thin-section seen in* ***7c****.*

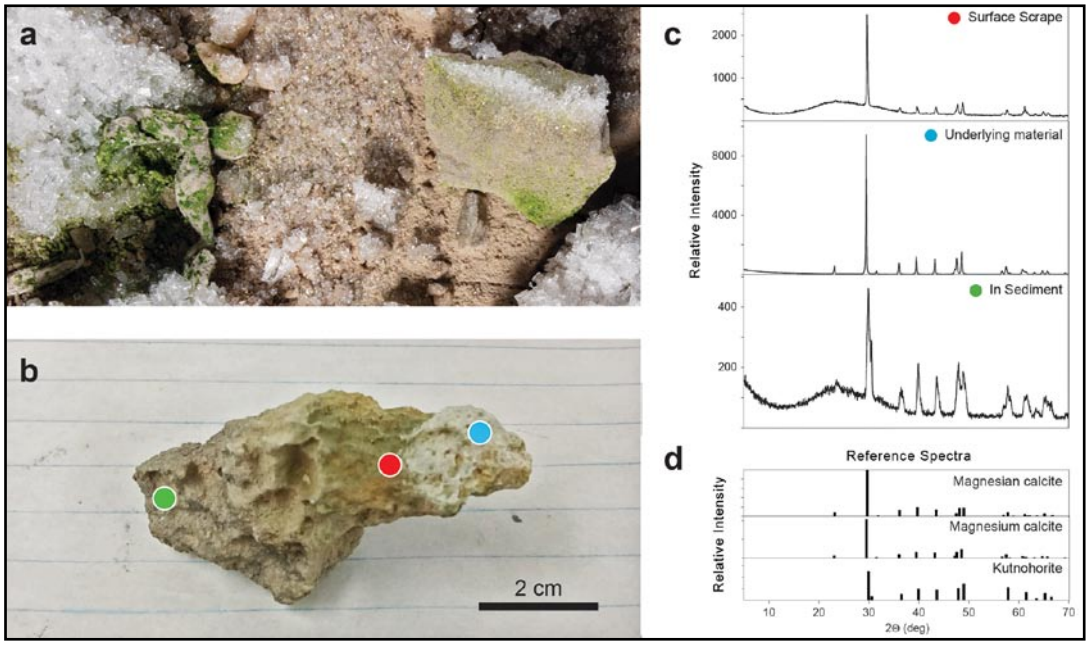

***Figure 8**: Green material associated with sediment clasts. The bright green material **(Fig.8a)** was identified as photosynthetic algae (Barton et al., 2020). Examination of the other material exposed on a single clast **(Fig8b)** using XRD **(Fig.8c)** revealed an interesting mineralogy. Pale green surface material (red dot) was scraped off, revealing a white limestone underneath (blue dot). Both this surface and underlying material were enriched in Mg^{2+} as magnesian calcite. An area of the same clast that had been buried in the sediment (green dot) revealed the presence of kutnohorite.*

***8c**: XRD spectra of tested samples.*

***8d**: Reference XRD spectra.*

airflow (U-Shaped and Cairn Climb), an ambient air temperature of approximately −3.0°C was measured, which is supported by the extensive growth of hexagonal crystals of hoar frost in Crystal Kingdom (Pounder, 1965). This temperature was used to constrain the upper limit for the caves at −3.0°C. Based on the data collected here, the ice floors, ice stalagmites, hoar frost horizon, sublimation horizon, and a measured isotherm indicate that air dynamics in these caves (Fig.3) remain active throughout the summer. In our model, based on a single-entrance cave (assuming no chimney effect), these cave-air dynamics are driven by the sub-freezing (permafrost) temperatures of the Grottedal caves (Fig.9).

Winter

During the winter, when the outside air temperature drops below the average cave temperature of −3.0°C, density-induced convection of cold air (or forced advection driven by the windy conditions of Grottedal) (Chiron and Loubière, 1988) causes colder surface air to drain into the cave, with a higher-level return of warmer cave air to the surface (Fig.9) (Wigley and Brown, 1976; Covington and Perne, 2015). This cold air is dry (due to the humidity capacity of cold air), causing sublimation of ice throughout the system (Fig.9), while cooling cave surfaces by convection (Wigley and Brown, 1976; Covington and Perne, 2015; Perşoiu and Lauritzen, 2018). Due to this cooling, and the higher density of this cold air, in a descending passage this creates a stable layer of cold air that remains throughout the summer, which also accounts for the preservation of ice deposits in many ice caves (Wigley and Brown, 1976; Smithson, 1991; Covington and Perne, 2015).

Summer

During the summer, warmer outside-air is cooled as it comes into contact with the below-freezing surfaces of the cave, where it loses moisture by the freezing of water vapour as hoar frost. This colder and now drier air has a higher density (calculated as 1.235kg/m^3 on the floor of Cove Cave), which sinks to the floor of the cave (Fig.9). This dry air is under-saturated with respect to water (absolute humidity calculated as 0.001kg/m^3), causing sublimation of ice encountered, including the floor ice and hoar frost, creating a boundary (or horizon) of sublimation (Fig.9). Caves with significant floor ice in the entrance tended to have higher levels of hoar frost, which suggests that the moisture could be picked up from the entrance ice. Caves with extensive hoar frost but no entrance ice, such as Crystal Palace, suggest that ice may have been present at the entrance before the study visits, or that this sublimation cycle is initiated by surface snow.

Sublimation increases the water vapour content of this air, decreasing its density and causing it to become buoyant. This lighter, wetter air (at 1.191kg/m^3 just above the thermocline in Cove Cave) rises, entering the warmer zone, where heating increases the volume and continues to reduce in density (measured as 1.182kg/m^3 at the ceiling of Cove Cave). This wetter air comes into contact with the sub-freezing rock surfaces, which leads to the formation of additional hoar frost (Harrison and Tiller, 1963; Pounder, 1965). If sufficiently close to the entrance, the warmer air begins to heat the surface of the rock, allowing the thawing of frost or condensation, and leading to the accumulation of floor ice and ice stalagmites (De Freitas and Schmekal, 2003; Gabrovšek *et al*., 2010). In either case, the air loses water vapour and cools, becoming denser and dropping into the colder, drier zones of the cave, supported by the decrease in relative humidity of the air close to the ceiling (Fig.4).

The cryogenic frostwork, which is found in distinct locations of the cave (on the entrance side of hoar frost), may indicate the location of a transition zone, where condensation and freezing are occurring on short (diurnal) cycles, while the magnesium/manganese calcites indicate the zone of condensation

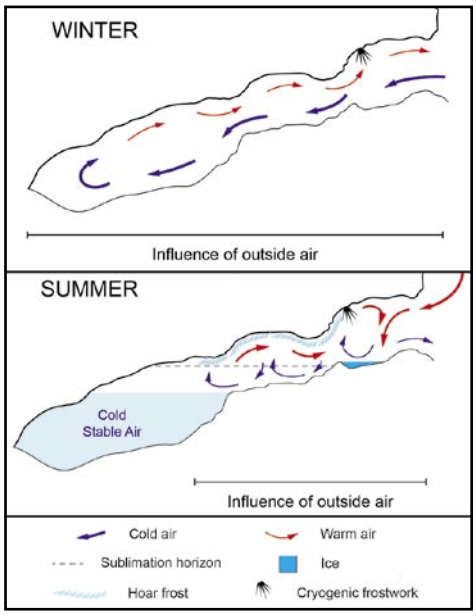

***Figure 9**: Model for cave airflow dynamics between summer and winter in the Grottedal caves. During winter, the outside air temperature drops, density-induced flow causes colder surface air to drain into the cave, pushing warmer cave out. This cold, dry air causes sublimation of ice throughout the system. The higher density of this cold air creates a stable layer of cold air in the cave during the summer, maintaining cooler cave temperatures. Humid, outside air is cooled and freezes as hoar frost as it comes into contact with the freezing surfaces of the cave, sinking to the floor. This colder, drier air sublimates the ice encountered. Sublimation increases the water vapour content of this air, decreasing its density and causing it to become buoyant. A sublimation horizon is then created, at the point where the warmer, humid air flows over the top of the cold, dense air. At locations close enough to the entrance, warmer surface air begins to heat the rock, allowing the thawing of frost and/or condensation. This transition zone may be indicated by the presence of condensation corrosion within the entrance zone, along with cryogenic frostwork.*

corrosion during the summer months. We suggest that a convective cycle that might be unique to caves within the permafrost zone is occurring within the Grottedal caves, the limits of which are defined by the hoar frost accumulations and sublimation horizons, along with the deposition of cryogenic frostwork and geochemical transformation of calcite surfaces. Additional work is required to confirm these findings, including a mechanism of action for the formation of the cryogenic frostwork, while also identifying several features that could be studied in similar caves found within permafrost zones.

Acknowledgements

This work was funded by the Austrian Science Fund (project no. Y 1162-N37). The Greenland government are thanked for permission to undertake this fieldwork (KNNO Expedition Permit C-19-32; Scientific Survey Licence VU-00150; Greenland National Museum and Archives 2019/01). The authors also thank the following individuals for helpful discussions during the preparation of this report: Paul Burger, Matt Covington, Derek C Ford, and Stein-Erik Lauritzen, as well as Bogdan Onac for providing critical feedback. Robbie Shone is thanked for the photographs used in Figs 2, 4, 5 and 6; Anika Donner and Manuela Wimmer are thanked for stable isotope preparation and analysis; and the other members of the Greenland Caves Project are thanked for providing in-field assistance. The authors are also grateful for the planning, logistics and transport support provided by Polog, Norlandair and Air Greenland. Additional information on the Greenland Caves Project can be found at: **Greenlandcavesproject.org**

References

Barton, H A, Breley, G J and Smith, M P, 2020. Microbiological observations in the caves of Grottedal, Kronprins Christian Land, northeastern Greenland. *Cave and Karst Science*, Vol.47(2), 88–92.

Behrendt, L, Trampe, E L, Nord, N B, Nguyen, J, Kühl, M, Lonco, D, Nyarko, A, Dhinojwala, A, Hershey, O S and Barton, H A, 2020. Life in the dark: far-red absorbing cyanobacteria extend photic zones deep into terrestrial caves. *Environmental Microbiology*, Vol.22(3), 952–963.

Bertozzi, B, Pulvirenti, B, Colucci, R R and Di Sabatino, S, 2019. On the interactions between airflow and ice melting in ice caves: A novel methodology based on computational fluid dynamics modeling. *Science of The Total Environment*, Vol.669, 322–332.

Box, J E, 2002. Survey of Greenland instrumental temperature records: 1873–2001. *International Journal of Climatology: a Journal of the Royal Meteorological Society*, Vol.22(15), 1829–1847.

Chiron, M and Loubière, J-F, 1988. Contribution to the study of the active layer in the area around Centrum Lake, northeast Greenland. *5th International Conference on Permafrost, Trondheim, Norway*.

Clark, I D and Lauriol, B, 1992. Kinetic enrichment of stable isotopes in cryogenic calcites. *Chemical Geology*, Vol.102, 217–228.

Covington, M D and Perne, M, 2015. Consider a cylindrical cave: A physicist's view of cave and karst science. *Acta Carsologica*, Vol.44(3), 363–380.

Davies, W E and Krinsley, D B, 1960. Caves in Northern Greenland. *Bulletin of the National Speleological Society*, Vol.22, 114–116.

De Freitas, C R and Schmekal, A, 2003. Condensation as a microclimate process: measurement, numerical simulation and prediction in the Glowworm Cave, New Zealand. *International Journal of Climatology*, Vol.23, 557–575.

Domínguez-Villar, D, Krklec, K, Pelicon, P, Fairchild, I J, Cheng H and Edwards, L R, 2017. Geochemistry of speleothems affected by aragonite to calcite recrystallization – Potential inheritance from the precursor mineral. *Geochimica et Cosmochimica Acta*, Vol.22, 310–329.

Donner, A, Töchterle P and Moseley G E, 2020. Basic meteorological observations in the Centrumsø region of northeast Greenland. *Cave and Karst Science*, Vol.47(2), 104–106.

Ford, D C, 1976. Evidences of multiple glaciation in South Nahanni National Park, Mackenzie Mountains, Northwest Territories. *Canadian Journal of Earth Sciences*, Vol.13, 1433–1445.

Ford, D C, Harmon, R S, Schwarcz, H P, Wigley, T M L and Thompson, P, 1976. Geo-hydrologic and thermometric observations in the vicinity of the Columbia Icefield, Alberta and British Columbia, Canada. *Journal of Glaciology*, Vol.16, 219–230.

Ford, D C and Williams, P, 2007. Ice in caves. 294–298 [Section 8.5, in Chapter 8, Cave Interior Deposits] *in* Ford, D C and Williams, P, *Karst Hydrology and Geomorphology*. [Chichester, UK: John Wiley and Sons.]

Gabrovšek, F, Dreybrodt, W and Perne, M, 2010. Physics of condensation corrosion in caves. 491–496 *in* Andreo, B, Carrasco, F, Durán, J J and LaMoreaux, J W (eds), *Advances in Research in Karst Media*. [Berlin and Heidelberg: Springer.]

Georgiadis, I, Chatzopoulou, K, Kantiranis, N, Ioakeimidis, I and Tsirambides, A, 2019. Petrography and provenance of floor sediments from the Loutra Almopias Cave (Pella, Macedonia, Greece). *International Journal of Speleology*, Vol.48(3), 237–248.

Harmon, R S, Atkinson, T C and Atkinson, J L, 1983. The mineralogy of Castleguard Cave, Columbia Icefields, Alberta, Canada. *Arctic and Alpine Research*, Vol.15, 503–516.

Harned, H S and Davis Jr, R, 1943. The ionization constant of carbonic acid in water and the solubility of carbon dioxide in water and aqueous salt solutions from 0 to 50°. *Journal of the American Chemical Society*, Vol.65, 2030–2037.

Harris, S A, 1979. Ice Caves and Permafrost Zones in Southwest Alberta. *Erdkunde*, Vol.33, 61–70.

Harrison, J D and Tiller, W A, 1963. Ice interface morphology and texture developed during freezing. *Journal of Applied Physics*, Vol.34, 3349–3355.

Hill, C A and Forti, P, 1997. *Cave Minerals of the World*. [Huntsville, AL: National Speleological Society.]

Holmlund, P, Onac, B P, Hansson, M, Holmgren, K, Mörth, M, Nyman M and Perşoiu, A, 2005. Assessing the palaeoclimate potential of cave glaciers: the example of the Scărişoara Ice Cave (Romania). *Geografiska Annaler: Series A, Physical Geography*, Vol.87, 193–201.

IAEA, 2015. Nord Greenland (Climate Records). *WISER: Water Isotope System for Data Analysis, Visualization, and Electronic Retrieval. NUCLEUS Information Resource Portal, International Atomic Energy Agency.* [**iaea.org/resources/nucleus-information-resources**].

Iepure, S, 2018. Ice Cave Fauna. 163–171 *in* Perşoiu, A and Lauritzen, S-E (eds), *Ice Caves*. [Amsterdam: Elsevier.]

Kawano, J, Shimobayashi, N, Miyake, A and Kitamura, M, 2009. Precipitation diagram of calcium carbonate polymorphs: its construction and significance. *Journal of Physics: Condensed Matter*, Vol.21(42): 425102, 6pp.

Kern, Z and Perşoiu, A, 2013. Cave ice – the imminent loss of untapped mid-latitude cryospheric palaeoenvironmental archives. *Quaternary Science Reviews*, Vol.67, 1–7.

Krinsley, D B, 1960. Limnological Investigations at Centrum So, Northeast Greenland. *Polarforschung*, Vol.30, 24–32.

Lauriol, B, Carrier, L and Thibaudeau, P, 1988. Topoclimatic zones and ice dynamics in the caves of the northern Yukon, Canada. *Arctic*, Vol.41(3), 215–220.

Lauriol, B, Prévost, C, Deschamps, É, Cinq-Mars, J and Labrecque, S, 2001. Faunal and archaeological remains as evidence of climate change in freezing caverns, Yukon Territory, Canada. *Arctic*, Vol.54, 135–141.

Lauritzen, S-E, 2006. Caves and speleogenesis at Blomstrandsøya, Kongsfjord, W. Spitsbergen. *International Journal of Speleology*, Vol.35, 37–58.

Lauritzen, S E and Lundberg, J, 2000. Meso- and micromorphology of caves. 408–426 *in* Klimchouk, A B, Ford, D C, Palmer, A N and Dreybrodt, W (eds), *Speleogenesis: Evolution of Karst Aquifers*. [Huntsville, AL: National Speleological Society.]

Luetscher, M and Jeannin, P Y, 2004. A process-based classification of alpine caves. *Theoretical and Applied Karstology*, Vol.17, 5–10.

Luetscher, M, Jeannin, P Y, and Haeberli, W, 2003. Energy fluxes in an ice cave of sporadic permafrost in the Swiss Jura mountains – concept and first observational results. 691–696 *in* Phillips, M, Springman, S M and Arenson, L U (eds), *Proceedings of the Eighth International Conference on Permafrost*. [Zurich: A A Balkema.]

Mavlyudov, B R, 2018. Geography of Cave Glaciation. 209–220 *in* Perşoiu, A and Lauritzen, S-E (eds), *Ice Caves*. [Amsterdam: Elsevier.]

Middelburg, J J, De Lange, G J and van Der Weijden, C H, 1987. Manganese solubility control in marine pore waters. *Geochimica et Cosmochimica Acta*, Vol.51, 759–763.

Moseley, G E, 2016. *Northeast Greenland Caves Project Expedition Report*. [Innsbruck, Austria: Northeast Greenland Caves Project.]

Moseley, G E, Edwards, R L, Cheng, H, Lu, Y and Spötl, C, 2016. Northeast Greenland Caves Project: first results from a speleothem-derived record of climate change for the Arctic. *Geophysical Research Abstracts*, Vol.18, EGU2016-11152.

Moseley, G E, Rosvold, J, Gotfredsen, A B, Hajdas, I, Gilg, O, Gregersen, K M, Spötl C and Edwards, R L, 2019. First pre-modern record of the Gyrfalcon (*Falco rusticolus*) in Northeast Greenland. *Polar Research*, Vol.38, 3539.

Moseley, G E, Barton, H A, Spötl, C, Töchterle, P, Smith, M P, Bjerkenås, S E, Blakeley, C, Hodkinson, P D, Shone, R C, Sivertsen, H C and Wright, M, 2020. Cave discoveries and speleogenetic features in northeast Greenland. *Cave and Karst Science*, Vol.47, No.2, 74–87.

Needleman, S M, 1960. Soil Science Studies at Centrum So, Northeast Greenland, 1960. *Polarforschung*, Vol.30, 33–41.

Perşoiu, A and Lauritzen, S-E (eds), 2018. *Ice Caves*. [Amsterdam: Elsevier.]

Perşoiu, A, Onac, B P, Wynn, J G, Blaauw, M, Ionita, M and Hansson, M, 2017. Holocene winter climate variability in Central and Eastern Europe. *Scientific Reports*, Vol.7, 1–8.

Pflitsch, A, Piasecki, J, Sawiński, T, Strug, K and Zelinka, J, 2006. Development and degradation of ice crystals sediment in the Dobšinská Ice Cave (Slovakia). 8–12 *in* Turri, S and Zelinka, J (eds), *2nd International Workshop on Ice Caves, Slovakia*. [Slovakia: Slovak Caves Administration.]

Pounder, E R, 1965. *The physics of ice*. [Oxford, UK: Pergamon.] 160pp.

Smith, M P, Higgins, A K, Soper, N J and Sønderholm, M, 2004. The Neoproterozoic Rivieradal Group of Kronprins Christian Land, eastern North Greenland. 29–39 *in* Higgins, A K and Kalsbeek, F (eds), *East Greenland Caledonides: stratigraphy, structure and geochronology*. [Copenhagen: Geological Survey of Denmark and Greenland Bulletin 6.]

Smith, M P and Rasmussen, J A, 2020. The geology of the Centrumsø area of Kronprins Christian Land, northeast Greenland, and lithological constraints on speleogenesis. *Cave and Karst Science*, Vol.47(2), 60–65.

Smithson, P A, 1991. Inter-relationships between cave and outside air temperatures. *Theoretical and Applied Climatology*, Vol.44, 65–73.

Soleymani, M, Ford, D C, Nakhaei, M and Nadimi, A, 2018. Ice Caves in Iran. 425–436 *in* Perşoiu, A and Lauritzen, S-E (eds), *Ice Caves*. [Amsterdam: Elsevier.]

Spötl, C, 2011. Long-term performance of the Gasbench isotope ratio mass spectrometry system for the stable isotope analysis of carbonate microsamples. *Rapid Communications in Mass Spectrometry*, Vol.25, 1683–1685.

Vaks, A, Gutareva, O S, Breitenbach, S F M, Avirmed, E, Mason, A J, Thomas, A L, Osinzev, A V, Kononov, A M and Henderson, G M, 2013. Speleothems reveal 500,000-year history of Siberian permafrost. *Science*, Vol.340, 183–186.

Vaks, A, Mason, A J, Breitenbach, S F M, Kononov, A M, Osinzev, A V, Rosensaft, M, Borshevsky, A, Gutareva, O S and Henderson, G M, 2020. Paleoclimate evidence of vulnerable permafrost during times of low sea ice. *Nature*, Vol.577, 221–225.

Van Tatenhove, F G M and Olesen, O B, 1994. Ground temperature and related permafrost characteristics in west Greenland. *Permafrost and Periglacial Processes*, Vol.5, 199–215.

Wigley, T M L and Brown, M C, 1976. The physics of caves. *The Science of Speleology*, Vol.3, 329–347.

Yang, S and Shi, Y, 2015. Numerical simulation of formation and preservation of Ningwu ice cave, Shanxi, China. *The Cryosphere*, Vol.9, 1983–1993.

Žák, K, Onac, B P and Perşoiu, A, 2008. Cryogenic carbonates in cave environments: A review. *Quaternary International*, Vol.187, 84–96.

Žák, K, Onac, B P, Kadebskaya, O, Filippi, M, Dublyansky, Y and Luetscher, M, 2018. Cryogenic Mineral Formation in Caves. 123–162 *in* Perşoiu, A and Lauritzen, S-E (eds), *Ice Caves*. [Amsterdam: Elsevier.]